iScience

CellPress
OPEN ACCESS

Article

ACKR4a induces autophagy to block NF-κB signaling and apoptosis to facilitate *Vibrio harveyi* infection

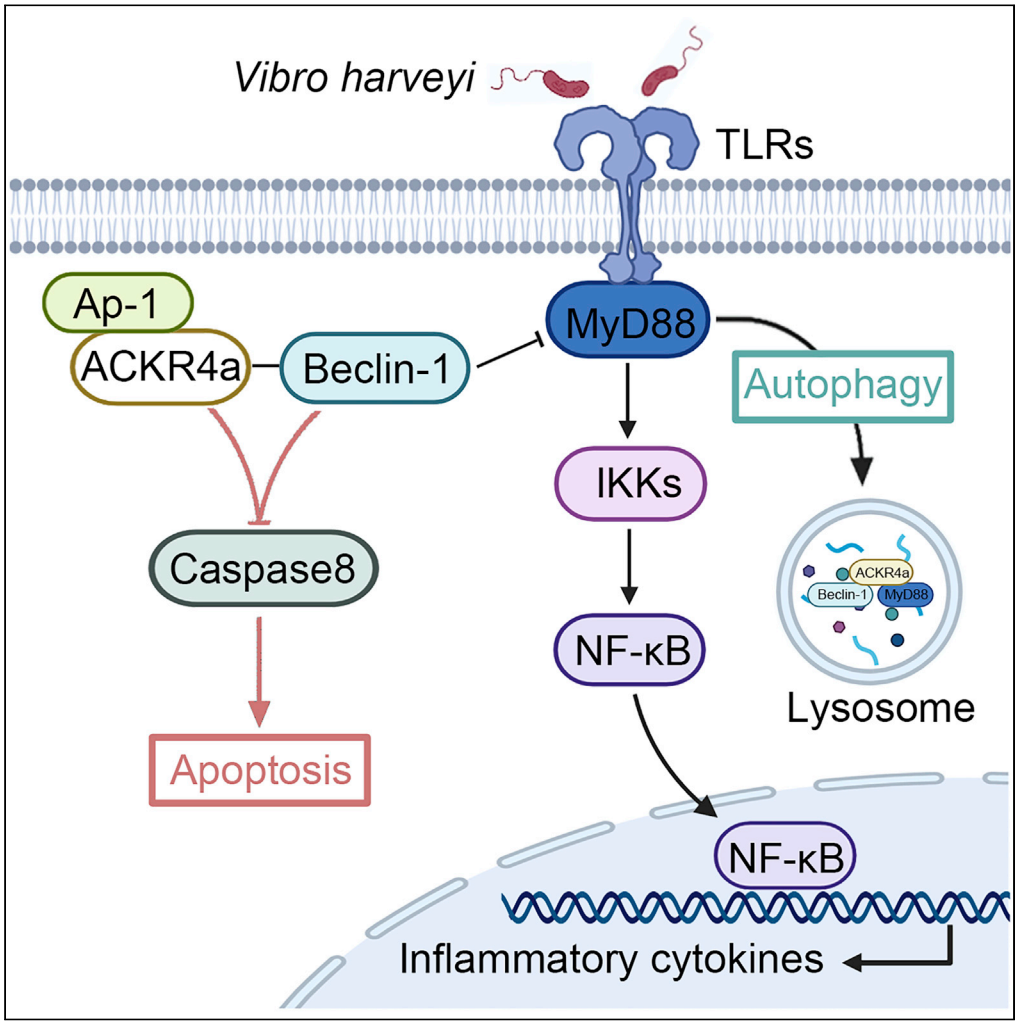

Ya Chen, Baolan Cao, Weiwei Zheng, Tianjun Xu

tianjunxu@163.com

Highlights

ACKR4a is a suppressor of NF-κB pathway

ACKR4a induced autophagy inhibits NF-κB signaling

ACKR4a up regulates Beclin-1 and induces autophagy to block apoptotic signaling

Chen et al., iScience *26*, 106105
March 17, 2023
https://doi.org/10.1016/j.isci.2023.106105

iScience

CellPress
OPEN ACCESS

Article

ACKR4a induces autophagy to block NF-κB signaling and apoptosis to facilitate *Vibrio harveyi* infection

Ya Chen,[1] Baolan Cao,[1] Weiwei Zheng,[1] and Tianjun Xu[1,2,3,*]

SUMMARY

Autophagy and apoptosis are two recognized mechanisms of resistance to bacterial invasion. However, bacteria have likewise evolved the ability to evade immunity. In this study, we identify ACKR4a, a member of an atypical chemokine receptor family, as a suppressor of the NF-κB pathway, which cooperates with Beclin-1 to induce autophagy to inhibit NF-κB signaling and block apoptosis, facilitating *Vibrio harveyi* infection. Mechanistically, *V. harveyi*-induced Ap-1 activates ACKR4a transcription and expression. ACKR4a forms a complex with Beclin-1 and MyD88, respectively, inducing autophagy and transporting MyD88 into the lysosome for degradation to suppress inflammatory cytokine production. Meanwhile, ACKR4a-induced autophagy blocks apoptosis by inhibiting caspase8. This study proves for the first time that *V. harveyi* uses both autophagy and apoptosis to evade innate immunity, suggesting that *V. harveyi* has evolved the ability to against fish immunity.

INTRODUCTION

The immune system is generally divided into innate and acquired immunity, with most organisms relying primarily on innate immunity for survival.[1] The innate immunity is a defense mechanism formed in organisms. It recognizes the pathogen-associated molecular pattern (PAMP) through the pattern recognition receptors (PRRs), makes a rapid response to pathogenic infection, and protects the host from infection.[2,3] As an important PRR, toll-like receptors (TLRs) can initiate a wide range of responses from phagocytosis to cytokine production, thereby further enhancing inflammatory and innate immune responses.[4] In most cases, TLRs signal primarily through a MyD88-dependent pathway, which transmits signals through cascade reactions to activate nuclear factor-kappa B (NF-κB).[5] NF-κB is one of the key factors in the initiation of innate immunity and is essential for the coordination of the inflammatory response, innate immunity, cell differentiation, proliferation and survival, and is considered to be the main initiator of the inflammatory response.[6] When bacteria infect the host, downstream effectors of the innate immune response such as cytokines and chemokines are synthesized, and ultimately lead to an inflammatory response to block the growth of bacteria. However, in coevolution with their hosts, bacteria have also developed various regulatory strategies to evade and subvert their host's defense.

Autophagy and apoptosis are thought to be the two important pathways against bacterial invasion.[7] Autophagy is a conservative process which transports abnormal proteins to lysosomes for degradation and plays an important role in innate immunity of eukaryotes against bacterial invasion.[8,9] However, some bacteria evade immunity by using autophagy in mammals. Normally, cells aim to remove invading extracellular bacteria and colonizing bacteria in the cytoplasm through autophagy,[10] but some bacteria are able to 'hijack' autophagy to complete self-growth and reproduction.[11–13] For instance, Unc-51-like kinase 1 (ULK1), Beclin1, microtubule-associated protein light chain 3 (LC3), and autophagy-related proteins (ATGs) cooperate to form autophagosomes, which encapsulate invading microorganisms and transport them to lysosomes for degradation.[14–16] However, *Mycobacterium tuberculosis* down-regulates Beclin-1 to prevent autophagosome formation, ultimately inhibiting autophagy and promoting infection.[17] In contrast with the inhibition of autophagosome formation, some bacteria use autophagosomes to complete self-replicating sites to promote proliferation.[11,18] In addition to autophagy, apoptosis is also a means of host defense against invading pathogens.[7]Apoptosis is a cell death pattern used to remove damaged cells to maintain the stability of the systemic environment.[19] On receiving a signal of bacterial invasion, the host induces apoptosis of infected cells

[1]Laboratory of Fish Molecular Immunology, College of Fisheries and Life Science, Shanghai Ocean University, Shanghai, China

[2]Laboratory of Marine Biology and Biotechnology, Qingdao National Laboratory for Marine Science and Technology, Qingdao, China

[3]Lead contact

*Correspondence: tianjunxu@163.com

https://doi.org/10.1016/j.isci.2023.106105

to inhibit bacterial infection.[20] Therefore, successful bacterial colonization depends on its ability to prevent apoptosis and protect bacterial replication. For instance, *Edwardsiella tarda* ensures its survival by inhibiting apoptosis after infection of zebrafish ZF4 cells,[21] *Shigella* achieves successful colonization by inhibiting apoptosis,[22] and S protein produced by group A streptococcus (GAS) binds to the erythrocyte membrane to evade detection of the host immune system.[23] Although many bacteria have been proved to have evolved the ability to evade immunity, there are a few reports in marine pathogens. *Vibrio harveyi* belongs to the Vibrionaceae family, which is recognized as a highly pathogenic agent of marine fish; it causes gastroenteritis, muscle necrosis, and skin ulcers, and is one of the main causes of marine fish mortality.[24]

Except for autophagy and apoptosis, some bacteria (e.g., *Staphylococcus aureus*) can even use their host's chemokine receptors to evade immunity.[25] Chemokine receptors are G protein-coupled receptors (GPCRs) found mainly on the surface of leukocytes. They contain seven transmembrane structures, which are involved in ligand binding and signaling, and play a key role in the initiation and maintenance of immune and inflammatory responses.[26] As chemokine research progressed, atypical chemokine receptors (ACKRs) were discovered.[27] Although ACKRs are structurally similar to other chemokine receptors and can internalize ligands, they cannot activate the signal transduction pathway because of the lack of the DRYLAIV domain, which is also called "silent receptor".[28] The function of ACKRs may be reflected in the following ways: 1. They can compete with typical receptors to bind chemokine, and thereby, regulate the signal transduction of cell chemotaxis; 2. By internalizing chemokine into cells, the concentration of chemokine in the environment is reduced to affect cell recruitment and act as a chemokine scavenger. 3. They assist chemokines to complete cross-cell transport through the stromal cell barrier.[29] The ACKRs family mainly including DARC,[30] D6 [31,32], CXCR7,[33] and CCRL1,[34] CCRL1 is also known as atypical chemokine receptor 4 (ACKR4). At present, some studies have shown that ACKR4 seems to realize signal transduction through the G protein independent pathway,[35–37] and it has non-redundant roles in controlling inflammation and immune response.[38] Its role in adaptive immunity is well known, but its function in innate immunity is rarely studied.

In innate immunity, the signal transduction of the TLR pathway is highly conserved from invertebrates to mammals. As a core protein of TLR signaling, MyD88 has been widely studied in vertebrates. In addition, because of the highly conserved structure of MyD88, its homologs in fish may have similar function to those in mammals.[39,40] In zebrafish, MyD88 has been shown to be involved in the clearance of bacterial infections.[41] Previous studies have also confirmed that *V. harveyi* evades immunity by destroying the signal transduction of MyD88.[42] However, the mechanisms of how *V. harveyi* evades immunity remain poorly understood in teleost fish. In this study, ACKR4a was rapidly up-regulated in *V. harveyi*-stimulated *Miichthys miiuy*. The up-regulated ACKR4a both suppressed innate immunity by inducing autophagy to block the MyD88-mediated NF-κB pathway, and inducing autophagy to block apoptosis, so as to enhance *V. harveyi* infection. To the best of our knowledge, this report is the first to elucidate that *V. harveyi* has been found to use both autophagy and apoptosis to evade innate immunity.

RESULTS

V. harveyi infection induces ACKR4a expression to promote self-proliferation

To identify genes that are potentially involved in the regulation of *V. harveyi* infection, we treated miiuy croaker with *V. harveyi* for 48 h, then used RNA-seq analysis to screen the different expression genes (DEGs) between *V. harveyi* treated and untreated spleen samples. From the deep-sequencing data, we identified 145 up-regulated genes and 280 down-regulated genes (Figure 1A). On this basis, we selected the 10 largest and 10 least DEGs (log2 of fold change was 1.0) for clustering heatmap, and the result showed that the respective samples in both the *V. harveyi* treated and untreated samples were well replicated (Figure 1B). The ACKR4a mRNAs were examined and found it was highly expressed in *M muiiy* brain after *V. harveyi* infection (Figure S1A). So the *M. muiiy* brain cell line (MBrC) was used for subsequent experiments. The knockdown efficiency of ACKR4a-si1 is 46.1% and ACKR4a-si2 is 63.7% in MBrC (Figure S1B), so ACKR4a-si2 (named ACKR4a-si) was used for subsequent experiments. Subsequently, we focused on the gene ACKR4a, which may have an immune function, and the colony-forming units (CFU) assay results revealed that ACKR4a promoted *V. harveyi* proliferation (Figures 1C, 1D, and S1C). To further investigate the mechanism by which ACKR4a promotes *V. harveyi* proliferation, the expression pattern of ACKR4a was analyzed. It is clear that ACKR4a in MBrC cells was regulated by *V. harveyi*. The results showed a time-dependent manner with *V. harveyi* infection at both mRNA and protein levels (Figures 1E and 1F). In addition, ACKR4a silencing effectively suppressed the expression of ACKR4a at both mRNA and protein levels (Figures 1E and 1G). The above results indicated that the up-regulation of ACKR4a may facilitate *V. harveyi* infection.

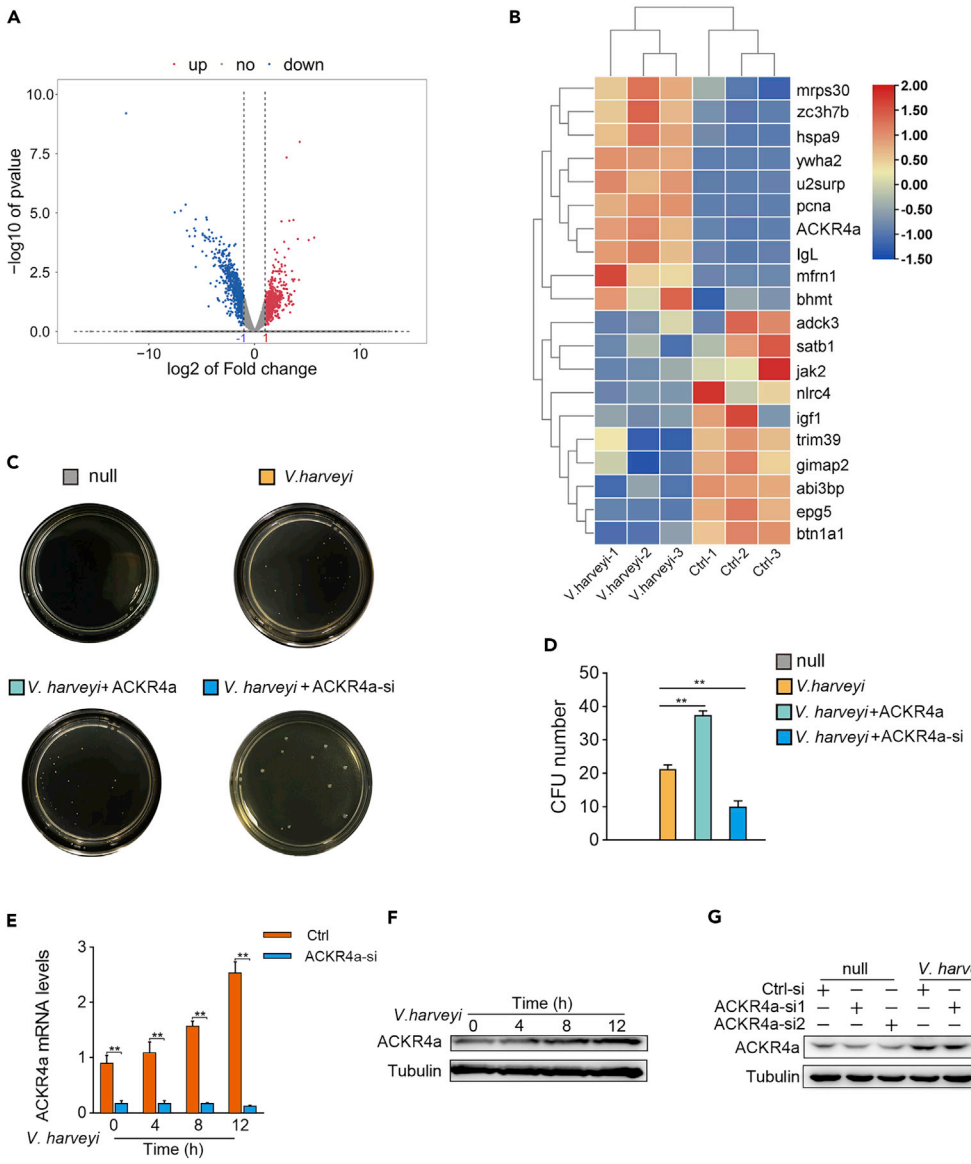

Figure 1. *V. harveyi*-induced ACKR4a facilitates its self-proliferation

(A) Volcano plot was drawn based on log2 of Fold change >1 for up-regulated genes and log2 of Fold change <1 for down-regulated genes.

(B) Heatmap was drawn with the RNA-sequencing data.

(C and D) Cells were transfected with ACKR4a or ACKR4a-si, lysates from *V. harveyi* infected cells were incubated on 2216E Agar plates for 12 h, and the colony forming unit (cfu) was counted.

(E) MBrC was transfected with Ctrl-si and ACKR4a-si, and then cells suffered *V. harveyi* infection for different times. ACKR4a mRNAs were detected by qPCR.

(F) MBrC suffered *V. harveyi* infection for different times and ACKR4a protein was detected by immunoblot.

(G) MBrC was transfected with Ctrl-si and ACKR4a-si, and then cells suffered *V. harveyi* infection. ACKR4a protein was detected by immunoblot. The data are shown as the mean ± SE of three independent experiments. (*) $p < 0.05$, (**) $p < 0.01$ versus the controls.

ACKR4a inhibits *V. harveyi*-triggered NF-κB signaling

We found that the rate of cell proliferation was affected when MBrC was infected with *V. harveyi*, and to verify this finding we performed cell proliferation assays. The results showed that *V. harveyi* infection did reduce the proliferation of MBrC (Figure S1D). Subsequent experiments have confirmed that ACKR4a over-expression reduced cell proliferation, whereas ACKR4a silencing enhanced cell proliferation (Figure 2A

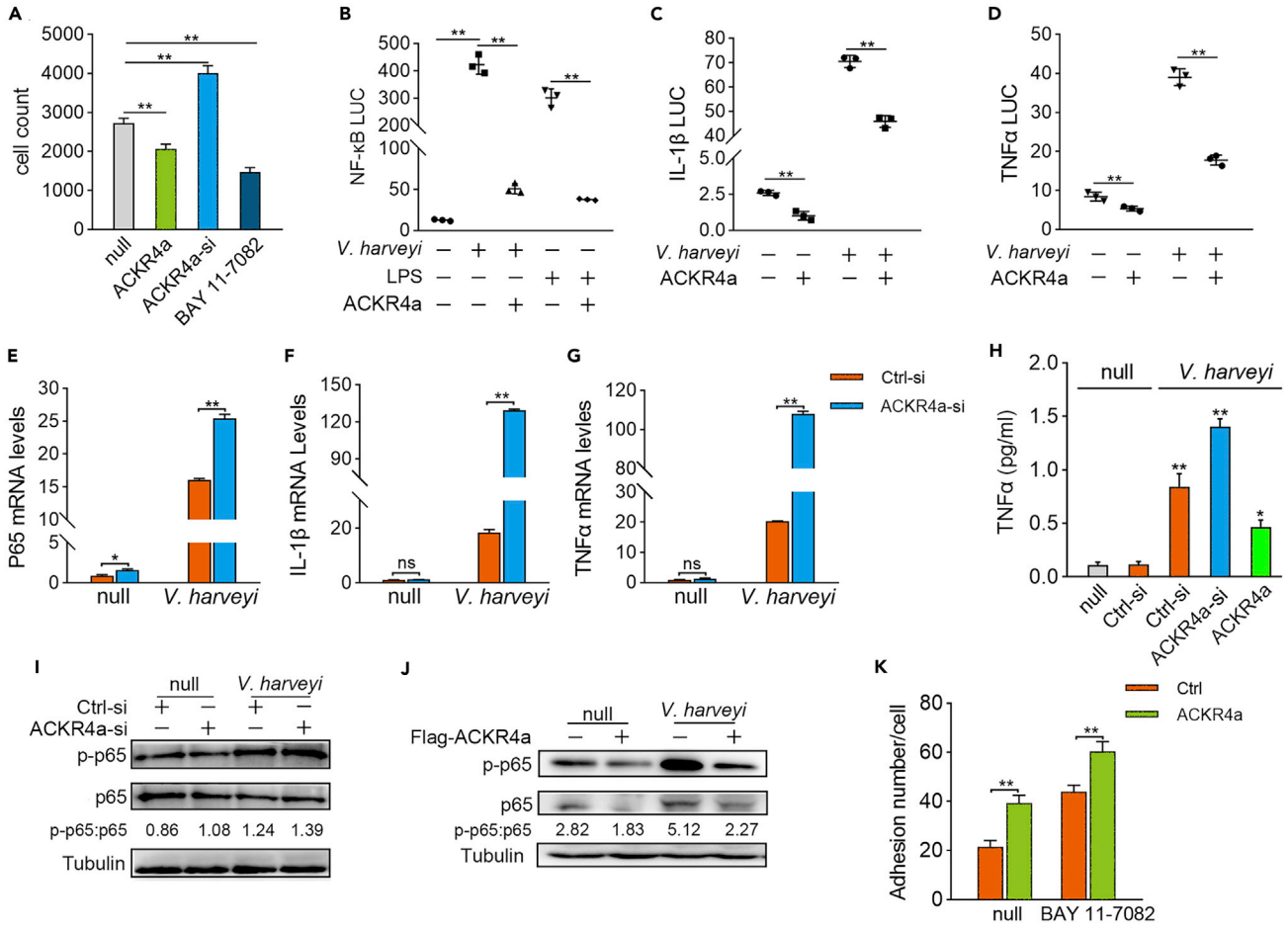

Figure 2. ACKR4a inhibits *V. harveyi*-triggered NF-κB signaling

(A) MBrC cells were transfected or treated with BAY 11–7082 for 24 h, and then infected with *V. harveyi* for 6 h before the cell proliferation assay, proliferating cells were counted.

(B–D) EPC cells were transfected with NF-κB, IL-1β, and TNFα reporter gene. Cells were treated with *V. harveyi* for an additional 12 h at 24 h after transfection followed by detection of luciferase activity.

(E–G) MBrC was transfected with ACKR4a-si or Ctrl-si and then treated with *V. harveyi* for an additional 12 h at 24 h after transfection. NF-κB, IL-1β, and TNFα mRNAs were analyzed by qPCR.

(H–J) (H) TNFα production was detected by ELISA in ACKR4a silenced and ACKR4a-overexpressed MBrC with *V. harveyi* infection for 24 h. MBrC was transfected with ACKR4a-si (I) or Flag-ACKR4a (J), and then cells were treated with *V. harveyi* for an additional 12 h at 24 h after transfection, subsequent to immunoblot detection of p65 phosphorylation.

(K) Cells were transfected with ACKR4a or treated with BAY 11–7082, lysates from *V. harveyi* infected cells were incubated on 2216E Agar plates for 12 h, and the colony forming unit (cfu) was counted. The data are shown as the mean ± SE of three independent experiments. (*) $p < 0.05$, (**) $p < 0.01$ versus the controls.

and S1E). Several studies have demonstrated that activation of NF-κB promotes cell proliferation. It was found that BAY 11–7082, the inhibitor of NF-κB, could also reduce the proliferation of MBrC (Figure 2A and S1E). Similar to previous reports,[43] the increase of NF-κB-luc was associated with the *V. harveyi* infection in a time-dependent manner (Figure S1F).

To further determine the effect of ACKR4a on *V. harveyi*-triggered NF-κB signaling, a luciferase reporter assay was performed. ACKR4a significantly inhibited *V. harveyi*- and LPS-triggered NF-κB luciferase activity; *V. harveyi*-triggered IL-1β and TNFα luciferase activity was also inhibited by ACKR4a (Figures 2B–2D). Endogenous ACKR4a was silenced to validate its role in the innate immunity. Then the expression patterns of p65 and pro-inflammatory cytokines (IL-1β and TNFα) were further detected, ACKR4a silencing drastically increased p65 mRNAs, IL-1β mRNAs, and TNFα mRNAs (Figures 2E–2G). The results in MLC and MKC also indicated ACKR4a could inhibit NF-κB signaling (Figures S1G–S1J). The ELISA results were

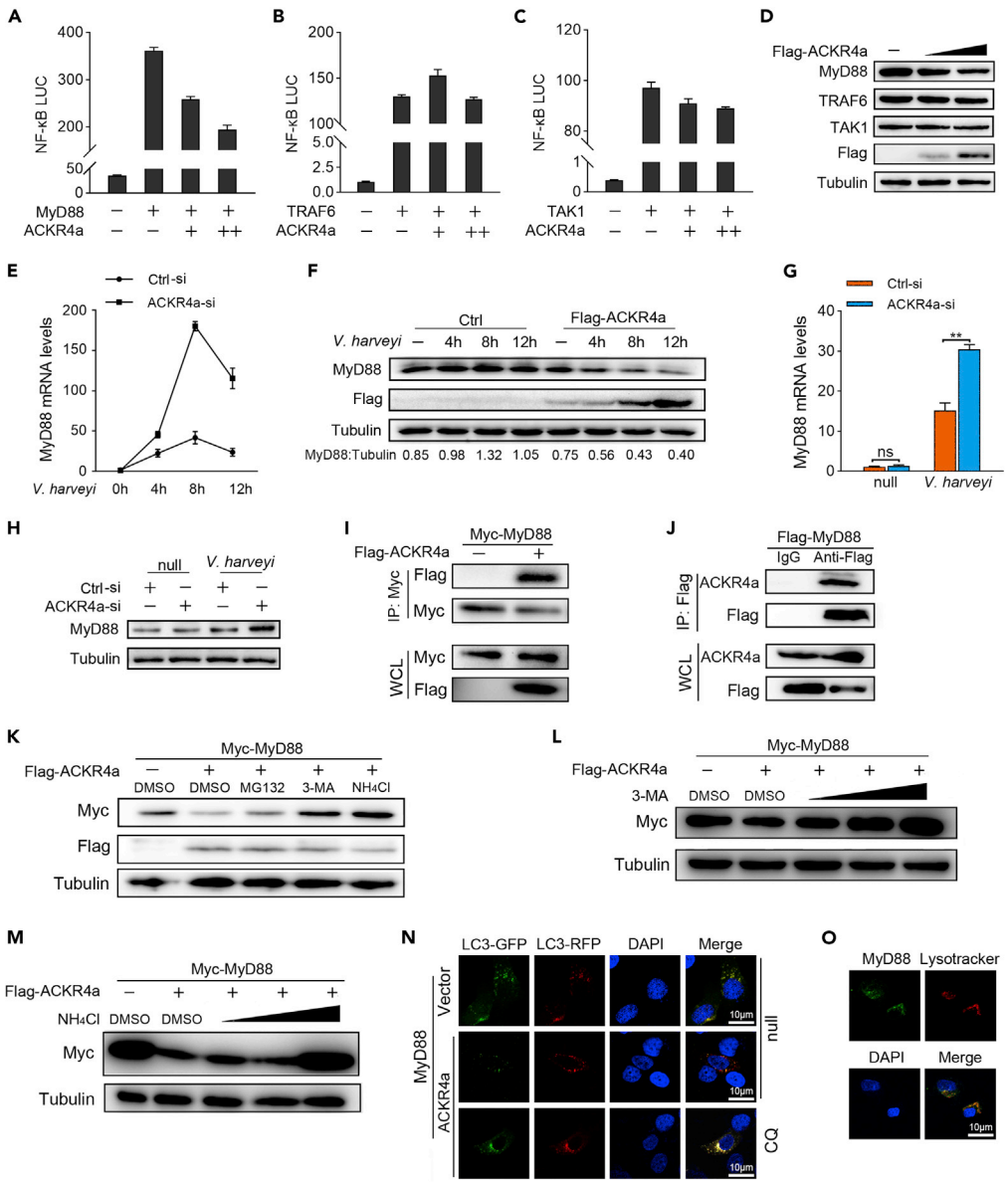

Figure 3. ACKR4a interacts with MyD88 and promoters MyD88 degradation in autophagy

(A–C) MBrC was transfected with indicated plasmids for 24 h, followed by detection of luciferase activity.

(D) MBrC was transfected with indicated plasmids for 24 h, followed by detection with immunoblot.

(E) MBrC was transfected with ACKR4a-si or Ctrl-si, the expression of MyD88 was determined by qPCR after *V. harveyi* infection for different times.

(F) MBrC was transfected with indicated plasmids, and then *V. harveyi* infected for different times, MyD88 was detected by immunoblot. MBrC was transfected with ACKR4a-si and treated with *V. harveyi* for an additional 12 h at 24 h after transfection, subsequent qPCR detection (G) and immunoblot detection of MyD88 (H).

(I) EPC cells were transiently transfected with Myc-MyD88 and Flag-ACKR4a, 36 h later, assessed before (WCL) or after (IP) immunoprecipitation with an antibody to Myc.

(J) Immunoblot analysis of interaction, EPC cells were transiently transfected with Flag-MyD88, 36 h later, assessed before (WCL) or after (IP) immunoprecipitation with an antibody to Flag.

(K) EPC cells were transfected with the indicated plasmids for 24 h, cells were stimulated with MG132 (10 μM), 3-MA (10 mM), or NH_4Cl (20 mM) for an additional 8 h, DMSO was as a negative control. MyD88 was detected and normalized to tubulin.

(L and M) EPC cells were co-transfected with the indicated plasmids for 24 h; dose escalation-3-MA or NH_4Cl was added for an additional 8 h. MyD88 was detected and normalized to tubulin.

Figure 3. *Continued*

(N) MBrC was co-transfected with MyD88, ACKR4a, and LC3-GFP-RFP for 24 h, and then cells were treated with CQ for 6 h. The nuclei were stained by DAPI (blue).

(O) MBrC was transfected with GFP-MyD88, 24 h later, cells were treated for 90min with the 50 nM LysoTracker red DND-99. The nuclei were stained by DAPI (blue). Pictures were taken by FCFM. Scale bar, 10 μm; original magnification ×40. The data are shown as the mean ± SE of three independent experiments. (*) $p< 0.05$, (**) $p< 0.01$ versus the controls.

also similar; ACKR4a silencing significantly increased TNFα and ACKR4a overexpression inhibited TNFα (Figure 2H). To evaluate the activation of NF-κB, it is more necessary to analyze the transliterated form, that is phosphorylated NF-κB, and it is a measure of NF-κB activity on target genes. On stimulation of NF-κB, p65 is phosphorylated and enters the nucleus to regulate the transcription of pro-inflammatory cytokines. To explore the regulation of p65 phosphorylation by ACKR4a, we measured the phosphorylation level of p65 after ACKR4a silencing and ACKR4a-overexpression by immunoblot. *V. harveyi* infection enhanced p65 phosphorylation, which proved that *V. harveyi* effectively activated NF-κB. On this basis, ACKR4a silencing enhanced p65 phosphorylation, whereas ACKR4a-overexpression decreased p65 phosphorylation, indicating that ACKR4a is an inhibitor of NF-κB signaling (Figures 2I and 2J). In zebrafish, the knockdown of ACKR4a increased the phosphorylation of p65. In addition, the CFU assay showed BAY 11–7082 significantly increase the proliferation of MBrC (Figure 2K). Overall, these data suggest that ACKR4a functions as a negative regulator of NF-κB signaling to inhibit the innate immunity during *V. harveyi* infection.

ACKR4a interacts with MyD88 and promotes MyD88 for autophagic degration

Next, we sought to determine which target in NF-κB signaling mediates ACKR4a's suppressive function. The NF-κB-luciferase reporter assay revealed that overexpression of ACKR4a caused a reduction of luciferase activity, which was induced by MyD88 in a dose-dependent manner (Figure 3A). However, overexpression of ACKR4a showed no effect on luciferase activity driven by TRAF6 or TAK1 (Figures 3B and 3C). An immunoblot result was similar to the luciferase reporter assay; overexpression of ACKR4a inhibited MyD88 in a dose-dependent manner, but there was no effect on TRAF6 and TAK1 (Figure 3D). These results suggest that ACKR4a functions at the MyD88 level.

All mammalian TLRs, with the exception of TLR3, depend at least in part on MyD88 adaptor to transmit signals, which makes direct regulation of MyD88 more effective.[44] We then examined the expression of MyD88 at different times of the *V. harveyi* infection and found ACKR4a silencing enhanced the expression of MyD88 (Figure 3E), and ACKR4a-overexpression inhibited MyD88 expression in a time-dependent manner (Figure 3F). An interesting result was found that although ACKR4a silencing enhanced MyD88 expression triggered by *V. harveyi*, this enhancement was not present when the cells were resting (Figures 3G and 3H). To better understand the molecular mechanism underlying the action of ACKR4a in the MyD88-mediated NF-κB signaling, we carried out the Co-immunoprecipitation (Co-IP) assays to determine whether ACKR4a interacts with MyD88. The Flag-ACKR4a could immunoprecipitate with Myc-MyD88 (Figures 3I and S1K). Consistent with that, we found that Flag-MyD88 could interact with endogenous ACKR4a (Figure 3J). Subsequent subcellular localization experiments showed ACKR4a had no significant co-localization with MyD88 (Figure S1L). Thus, these findings support the concept that ACKR4a physically interacts with MyD88, and their interaction likely occurs in the cytoplasm. Next, we investigated the mechanism by which ACKR4a suppressed MyD88 expression. Either NH_4Cl or 3-Methyladenine (3-MA), inhibitors of the autophagy-lysosome-dependent degradation pathway, resulted in a significant accumulation of MyD88 in the presence of ACKR4a, and MG132 did not affect the degradation of MyD88 (Figure 3K). Moreover, similar results showed that 3-MA and NH_4Cl significantly blocked MyD88 degradation in a dose-dependent manner (Figures 3L and 3M). These findings seem to suggest that blocking the autophagy effectively prevents ACKR4a-targeted MyD88 degradation. Autophagic flux denotes the dynamic process of autophagy, which is a reliable indicator of autophagic activity. Because GFP fluorescence is quenched in the lysosome, the stage of autophagy can be determined from the fluorescence of GFP and RFP.[42] Observation of the yellow fluorescence in the Merge panel showed more red fluorescence in the presence of ACKR4a, indicating ACKR4a promoted the fusion of autophagosomes and lysosomes; whereas the autophagy inhibitor chloroquine (CQ) prevented the fusion of autophagosomes and lysosomes, showing more yellow fluorescence (Figure 3N). To further validate that ACKR4a targets MyD88 for autophagic degradation, a lysosomal localization assay was performed, MyD88 (green) and lysosomes (red) were co-localized in MBrC cell (Figure 3O), suggesting

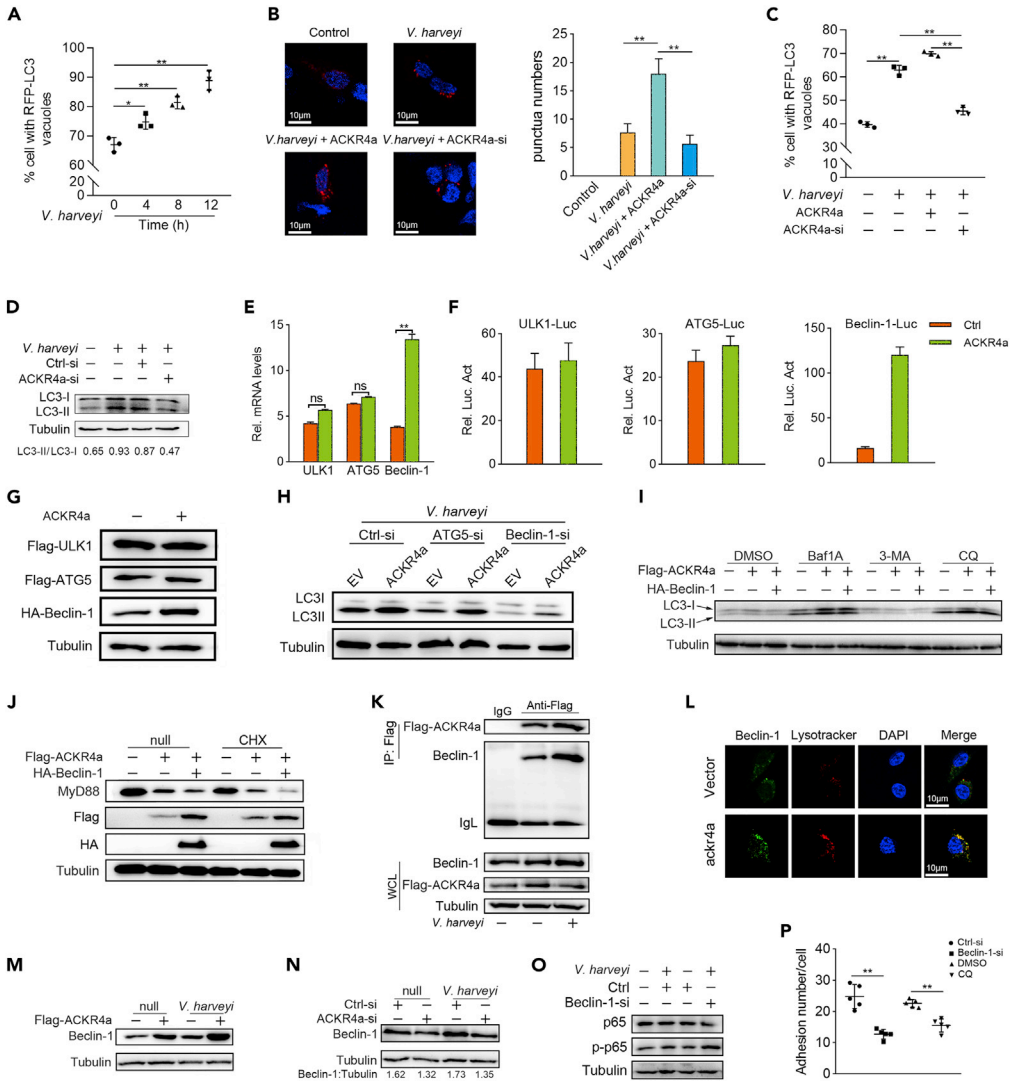

Figure 4. ACKR4a participates in the regulation of autophagy via Beclin-1

(A) MBrC was transfected with RFP-LC3 and then treated with *V. harveyi* at the indicated time. The extent of autophagy was assessed by analyzing staining patterns of RFP-LC3, and quantitation of autophagy was shown.

(B) MBrC was transfected with Flag-ACKR4a or ACKR4a-si, together with RFP-LC3. 24 h later, cells were infected with *V. harveyi*, and the percentage of cells with RFP-LC3 puncta was quantified (C).

(D) MBrC was transfected with ACKR4a-si or Ctrl-si. 24 h later, cells were infected with *V. harveyi* for 12 h. The positions of LC3-I and LC3-II were indicated.

(E) Cells were transfected the indicated plasmids for 36 h. ULK1, ATG5 and Beclin-1 mRNAs was detected by qPCR.

(F) MBrC was transfected with indicated plasmids for 24 h, followed by detection of luciferase activity.

(G) MBrC was transfected with indicated plasmids for 36 h, and then the immunoblot assay was performed.

(H) MBrC was transfected with Ctrl-si, ATG5-si and Beclin-1-si for 24 h, and then *V. harveyi* infected for an additional 6 h; the immunoblot assay was performed.

(I) EPC cells were co-transfected with the indicated plasmids for 24 h, cells were stimulated with Baf1A (10 μM), 3-MA (10 mM), or CQ (50 μM) for an additional 8 h, DMSO was as a negative control. LC3-I and LC3-II were detected and normalized to Tubulin.

(J) EPC cells were co-transfected with the indicated plasmids for 24 h, cells were infected with *V. harveyi* for 12 h. MyD88 was detected and normalized to Tubulin.

(K) EPC cells were transfected with Flag-ACKR4a for 24 h, then cells were infected with *V. harveyi*. 12 h later, assessed before (WCL) or after (IP) immunoprecipitation with antibody to Flag.

(L) MBrC was transfected with GFP-Beclin-1, 24 h later, cells were treated for 90 min with the 50 nM LysoTracker red DND-99. The nuclei were stained by DAPI (blue). MBrC was transfected with Flag-ACKR4a (M) or ACKR4a-si (N), 24 h later, cells were infected with *V. harveyi* for 12 h. Beclin-1 was detected and normalized to Tubulin.

Figure 4. *Continued*

(O) MBrC was transfected with ACKR4a-si or Ctrl-si. 24 h later, cells were infected with *V. harveyi* for 12 h, subsequent immunoblot detection of p65 phosphorylation.

(P) Cells were transfected with Beclin-1-si, treated with CQ or DMSO, lysates from *V. harveyi* infected cells were incubated on 2216E Agar plates for 12 h, and the colony forming unit (cfu) was counted. Pictures were taken by FCFM. Scale bar, 10 μm; original magnification ×40. The data are shown as the mean ± SE of three independent experiments. (*) $p < 0.05$, (**) $p < 0.01$ versus the controls.

MyD88 was transported to lysosomes. Taken together, these results suggest that ACKR4a interacts with MyD88 and targets MyD88 for autophagic degradation.

ACKR4a participates in the regulation of autophagy via Beclin-1

Some bacteria use autophagy to promote their growth and infection, their replication will be reduced when autophagy is absent.[13] To test whether *V. harveyi* participates in the regulation of autophagy in MBrC cells, cells were infected with *V. harveyi* and then the expression pattern of LC3 was examined. In MBrC cells, *V. harveyi* exposure increased the autophagy as indicated by the accumulation of GFP-LC3 puncta, which was accompanied by a time-dependent increase of *V. harveyi* infection (Figure 4A). ACKR4a overexpression enhanced *V. harveyi*-induced autophagy as shown by a remarkable increase in puncta accumulations of RFP-LC3, in contrast to ACKR4a silencing which significantly reduced *V. harveyi*-induced autophagy (Figures 4B and 4C). In addition, ACKR4a silencing resulted in a reduction in *V. harveyi*-induced LC3-II expression (Figure 4D).

ULK1, Beclin-1 and ATG5 were the key regulatory proteins of autophagy. qPCR results showed that ACKR4a significantly enhanced the expression of Beclin-1, but not ULK1 and ATG5 (Figure 4E). The luciferase reporter assay of ULK1, ATG5 and Beclin-1 revealed that overexpression of ACKR4a only caused an increase of Beclin-1luciferase activity (Figure 4F). Next, we detected that overexpression of ACKR4a enhanced the expression of Beclin-1, but not ULK1 and ATG5 (Figure 4G). Also, ACKR4a induced autophagy was inhibited by Beclin-1-si, whereas ATG5-si only has partially inhibition (Figure 4H). The above results indicated that ACKR4a was targeted on Beclin-1. Therefore, the function and mechanism of Beclin-1 in ACKR4a-mediated autophagic degradation of MyD88 were investigated. In zebrafish infected with *V. harveyi*, knockdown of ACKR4a did not result in significant changes in ULK1 while significantly reducing Beclin-1 and ATG5 (Figures S2B–S2D). Beclin-1 further enhanced ACKR4a-induced autophagic flux with Baf1A and CQ treated (Figure 4I), and Beclin-1 enhanced the degradation of MyD88 by ACKR4a (Figure 4J). We then carried out the Co-IP assays to determine whether ACKR4a interacts with Beclin-1, and found that ACKR4a interacts with Beclin-1, and *V. harveyi* infection enhanced the interaction between ACKR4a and Beclin-1 (Figure 4K). A lysosomal localization assay indicated that ACKR4a enhanced the autophagosome fuse with lysosome (Figure 4L). Subsequently, ACKR4a increases endogenous Beclin-1 expression (Figure 4M) and ACKR4a silencing attenuates *V. harveyi*-induced Beclin-1 expression (Figure 4N). In addition, Beclin-1 silencing enhanced the phosphorylation of p65 triggered by *V. harveyi*, which further suggests that *V. harveyi* induces autophagy to negatively regulate NF-κB signaling (Figure 4O). We next sought to determine the biological importance of Beclin-1 in *V. harveyi* infection, particular in controlling *V. harveyi* proliferation. The CFU assay was performed and found both Beclin-1 silencing and CQ-blocked autophagy reduced the proliferation of *V. harveyi*, which proves that *V. harveyi* utilize autophagy to promote its own proliferation (Figure 4P). The above results together reveal that ACKR4a induces and forms complexes with Beclin-1 to promote autophagy, and then facilitate *V. harveyi* infection.

ACKR4a induced autophagy to blocked apoptosis

Autophagic cell death is considered a reasonable alternative to apoptosis, and apoptosis is also a recognized antibacterial mechanism; successful bacterial infections complete self-replication by inhibiting apoptosis.[22] To determine the relationship between *V. harveyi*-induced autophagy and apoptosis, the apoptosis of MBrC cells with different treatments before and after *V. harveyi* infection were determined, and ACKR4a silencing increased *V. harveyi*-induced apoptosis (Figures 5A and 5B, the left panel). Because caspase3 and caspase7 are important in the initiation of apoptosis, they are widely accepted as reliable indicators of apoptosis. A caspase Glo 3/7 assay showed that ACKR4a overexpression inhibited *V. harveyi*-induced caspase3/7 activity, whereas ACKR4a silencing enhanced *V. harveyi*-induced caspase3/7 activity (Figure 5B, right panel). *V. harveyi* and exogenously added recombinant active caspase8 induced caspase3/7 activity was inhibited by ACKR4a (Figure 5C), suggesting that ACKR4a is capable of efficiently blocking apoptosis signaling. Although the ACKR4a induced autophagy has been demonstrated, further studies are needed to investigate the role of autophagy in blocking apoptosis. As shown in Figure 5D

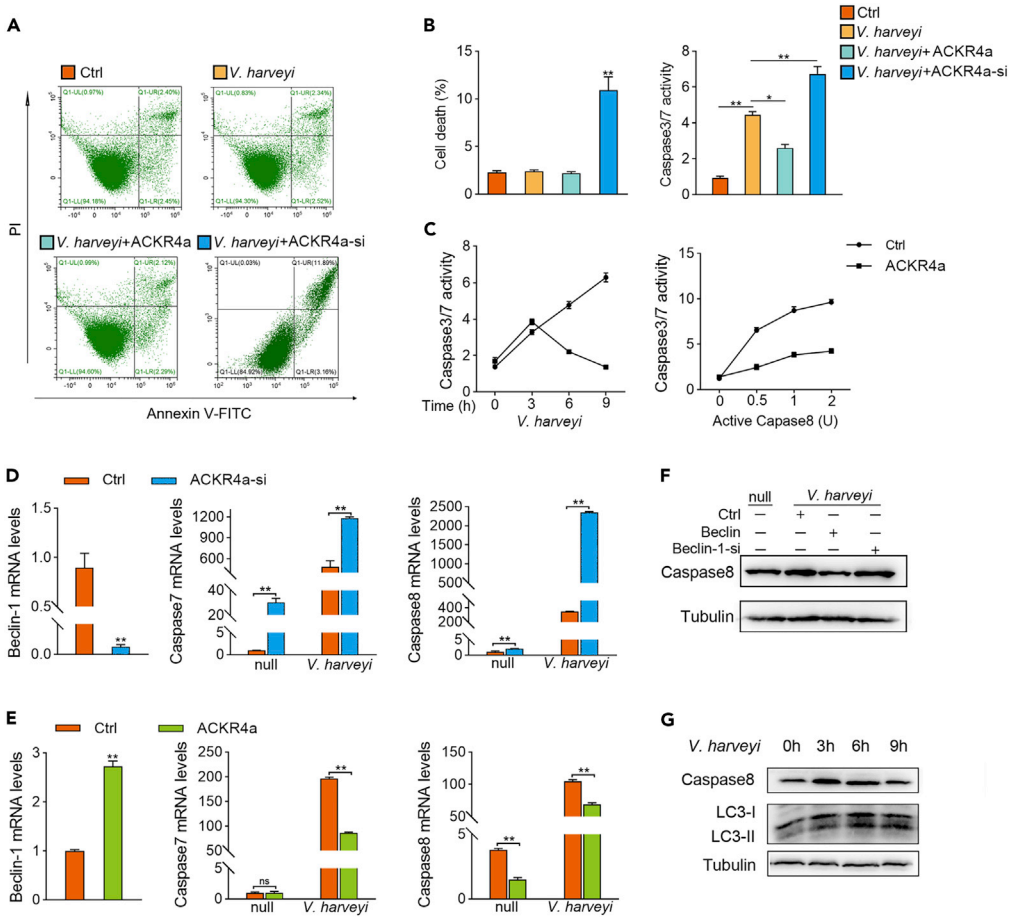

Figure 5. ACKR4a induces autophagy to block apoptosis

(A) Cells were stained with PI and Annexin-V-FITC, and the positively stained cells were counted using FACScan (B, left panel). (B, right panel) For caspase activity, 100μL/well of caspase 3/7 working solution was added and then incubates for 1 h at 25°C, protected from light. The plate was centrifuged at 800 g for 2 min, with fluorescence intensity monitoring at Ex/Em = 490/525 nm

(C) MBrC was transfected with ACKR4a, 24 h later, cells were treated with *V. harveyi* for different or activity caspase8 for different dosage. Then the caspase activity assay was performed. MBrC was transfected with ACKR4a plasmid and ACKR4a-si. 24 h later, cells were infected with *V. harveyi*, and qPCR assays (D and E) and immunoblot assay (F) were performed.

(G) MBrC was infected with *V. harveyi* for different times, and the caspase8 and LC3 were detected by immunoblot. The data are shown as the mean ± SE of three independent experiments. (*) $p < 0.05$, (**) $p < 0.01$ versus the controls.

ACKR4a silencing significantly increased the effector caspases (caspase7) and the initiator caspases (caspase8). In addition, ACKR4a overexpression inhibited caspase7 and caspase8 mRNAs (Figure 5E) and ACKR4a knockdown significantly increased caspase7 and caspase8 in zebrafish (Figures S2E and S2F). Previous studies have shown that Beclin-1 is a molecular switch that mediates apoptosis and autophagy processes,[45] so the involvement of Beclin-1 in the regulation of apoptosis was explored. In our study, Beclin-1 overexpression down-regulated *V. harveyi* induced caspase8, whereas Beclin-1 silencing up-regulated *V. harveyi* induced caspase8 (Figure 5F). An interesting result was found that caspase8 was significantly up-regulated at 3 h of *V. harveyi* infection; it was again inhibited with increasing duration of infection, and LC3-II was negatively correlated with caspase8 (Figure 5G). According to the above results, ACKR4a induced autophagy to block apoptotic signaling and facilitate *V. harveyi* infection, and Beclin-1 might be a potential target in the cascade of autophagy and apoptosis.

Ap-1 enhances ACKR4a induced autophagy at *V. harveyi* infection

Subsequently, the mechanism of *V. harveyi* infection-induced ACKR4a expression was investigated. Four different ACKR4a promoter plasmids were constructed first according to the promoter prediction

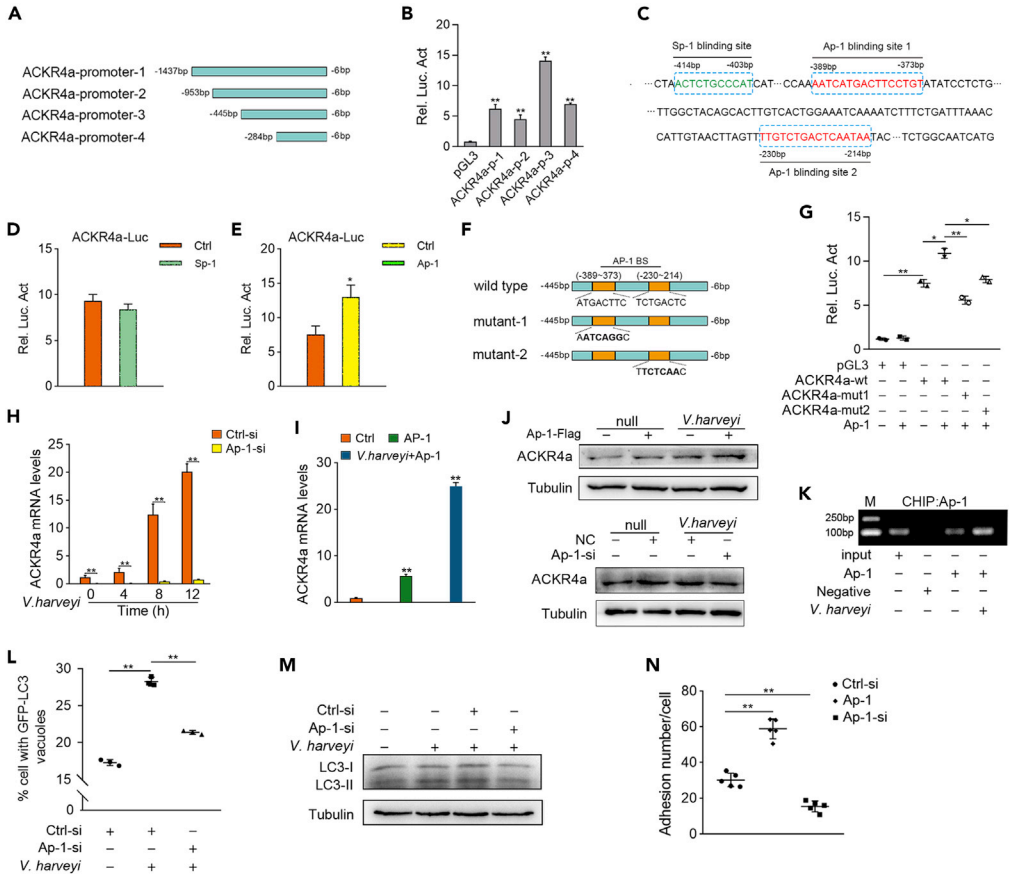

Figure 6. Ap-1 enhanced ACKR4a induced autophagy at *V. harveyi* infection

(A) According to the ACKR4a promoter prediction sequences, the promoters of different lengths were constructed into the PGL3-Basic reporter plasmid.

(B) EPC cells were transfected with the different promoters, and the luciferase actively was performed.

(C) Analysis of possible transcription factor binding sites in ACKR4a based on the promoter gene sequence of this sequence.

(D and E) MBrC was transfected with indicated plasmids for 24 h, followed by detection of luciferase activity.

(F) ACKR4a promoter region contains the potential Ap-1binding sites.

(G) Ap-1 promotes ACKR4a promoter activity. EPC cells were transfected with the indicated plasmid for 24 h, and then the luciferase activity was assayed. MBrC was transfected with Ap-1-si or Ap-1 plasmid. 24 h later, cells were infected with *V. harveyi* for different times. Then a qPCR assay (H and I) and immunoblot (J) were performed.

(K) ChIP analysis of Ap-1 binding to the promoter of ACKR4a. MBrC was treated with *V. harveyi* at the indicated time. ChIP was performed with Flag-Ap-1 antibody.

(L) MBrC was transfected with GFP-LC3, AP-1-si. 24 h later, cells were treated with *V. harveyi*. The percentage of cells with GFP-LC3 puncta was quantified.

(M) MBrC was treated as described in (L). The positions of LC3-I and LC3-II are indicated.

(N) Cells were transfected with Ap-1 or Ap-1-si, lysates from *V. harveyi* infected cells were incubated on 2216E Agar plates for 12 h, and the colony forming unit (cfu) was counted. The data are shown as the mean ± SE of three independent experiments. (*) $p < 0.05$, (**) $p < 0.01$ versus the controls.

sequences (Figure 6A). The luciferase assay showed that ACKR4a-p-3 activity was the highest (Figure 6B). To identify the upstream activator of ACKR4a expression during *V. harveyi* infection, the promoter region of ACKR4a was analyzed and found that ACKR4a has potential binding sites of Sp-1 and Ap-1 (Figure 6C). The ACKR4a-luc assay showed that Sp-1 could not enhance the luciferase activity and Ap-1 enhanced the luciferase activity (Figures 6D and 6E), which raised the possibility that ACKR4a could be a direct target of Ap-1. To examine this, two luciferase vectors consisting of mutant ACKR4a were constructed (Figure 6F). The luciferase assay showed that mutants lacking Ap-1 binding site inhibited the luciferase activity in contrast to wild-type (Figure 6G). To confirm that Ap-1 promotes ACKR4a expression, we silenced or enhanced the expression of Ap-1 via overexpression or knockdown and ACKR4a expression was assessed in transfected

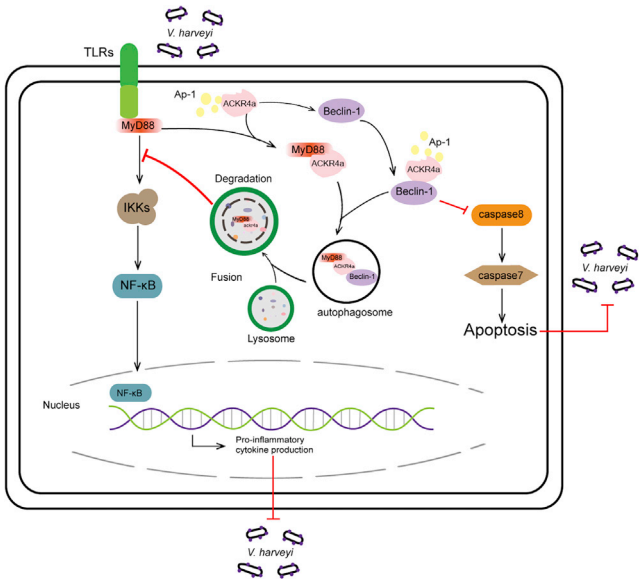

Figure 7. A working model of how ACKR4a facilitates *V. harveyi* infection

MBrC cells. Ap-1 silencing significantly reduced *V. harveyi*-induced ACKR4a expression (Figure 6H), whereas Ap-1 overexpression significantly enhanced ACKR4a expression (Figure 6I). The immunoblot results were consistent with the qPCR results, Ap-1 overexpression increased the expression of ACKR4a, whereas Ap-1 silencing decreases the expression of ACKR4a (Figure 6J). ChIP analysis showed that Ap-1 binds to the ACKR4a promoter in MBrC cells under normal physiological conditions, and *V. harveyi* stimulation enhanced the binding of Ap-1 to the ACKR4a promoter (Figure 6K). The above results confirmed that ACKR4a is a potential transcriptional target of Ap-1. The function of Ap-1 in autophagy was then explored; Ap-1 silencing effectively reduced the *V. harveyi* infection-induced accumulation of GFP-LC3 (Figure 6L), and it is also attenuated *V. harveyi* infection-induced up-regulation of LC3-II (Figure 6M). The CFU assay was performed to explore the role of Ap-1 in *V. harveyi* infection, and found that AP-1 facilitates *V. harveyi* proliferation (Figure 6N). Taken together, the above results indicated that Ap-1 activates ACKR4a transcription and expression and contributes to the *V. harveyi* infection.

DISCUSSION

ACKRs has been shown to be involved in several biological processes such as chemokine system regulation, chemokine ligand internalization, intracellular degradation and inflammatory response,[4,26] which is important not only for adaptive immunity, but also as an important component of innate immune system.[33,34] However, the role of ACKRs in the inflammatory response to bacterial infection in fish has not been investigated. This study demonstrates for the first time that ACKR4a, a member of ACKRs family, promotes the infection of *V. harveyi* to teleost fish through autophagy and apoptosis. Mechanistically, the transcription of ACKR4a was up-regulated by the transcription factor AP-1. Then the up-regulated ACKR4a was synergized with Beclin-1 to induce autophagy and transported MyD88 to lysosomes for degradation. Meanwhile, ACKR4a induces autophagy to blocked apoptosis, and then facilitated *V. harveyi* infection (Figure 7). Innate immunity plays a crucial role in protecting eukaryotes from endogenous and exogenous pathogenic invasion.[46] As a result of long-term exposure to microorganisms, fish have evolved more optimized innate immunity to protect them from infection.[47] TLRs recognized PAMP when bacterial infection occurs, and initiated an innate immune response via MyD88-dependent and independent pathways, which induced the production of pro-inflammatory cytokines to eliminate bacterial infection. MyD88 is an essential adaptor in TLR signaling, with the exception of TLR3, all mammalian TLRs utilize MyD88 to activate NF-κB signaling.[48] Therefore, it may be the most effective to directly regulate MyD88. For example, S-1-penylcysteine inhibits IL-6 production by inducing the degradation of MyD88. Similarly in fish, IRF3 and eIF3k have been reported to inhibit NF-κB signaling by targeting MyD88.[42,49] Accumulated evidence has also suggested that MyD88 was important for the elimination of bacterial infections. For instance, MyD88-deficient mice could not recognize the bacterial components and were

highly susceptible to *S. aureus*.[50] In addition, MyD88 has also been shown to be involved in the elimination of bacterial infections in zebrafish.[41] The activation of the innate immune system promotes bacterial clearance, which constitutes a major selective pressure, promoting them to evolve the ability to suppress innate immunity.[51,52] It has been demonstrated that salmonella can regulate immune response and manipulate inflammatory responses after infect host cells. The salmonella virulence *SpvC* irreversibly dephosphorylates ERK, p38, and MAPK, thereby inhibiting the transcription of pro-inflammatory cytokines.[53] In this study, the up-regulated ACKR4a in *V. harveyi* infected *M. miiuy* was combined with MyD88 to inhibit p65 phosphorylation and blocked NF-κB signaling. This suggests that bacteria can also suppress the innate immunity of fish by interfering with the stability of adaptor in the TLR signaling for the purpose of immune evasion.

Autophagy and apoptosis are two recognized mechanisms of resistance to bacterial invasion, with antimicrobial autophagy being a barrier against invading microorganisms. PRRs can induce autophagy at different stages of host-bacteria contact, and inhibit the intracellular growth of bacteria.[54] Conversely, bacteria have also evolved efficient mechanisms to prevent, combat or commandeer autophagy. These mechanisms often involve targeting Beclin-1 to block autophagy,[55] preventing the maturation of autophagosomes[56] and even activating autophagy in some cases to provide nutrition for bacterial growth.[57] Differently, we found that *V. harveyi* induced Beclin-1-activated autophagy via ACKR4a, which targets MyD88 for autophagic degradation, thereby blocking NF-κB signaling and promoting self-replication. Another defense strategy is the programmed cell death (apoptosis), which is activated when pathogens use host cells for survival and replication. For instance, mycobacterium infection of macrophages causes apoptosis, which contributes to the elimination of bacteria form cells.[58] In addition, TNF-α-mediated macrophages apoptosis destroys the intracellular environment for mycobacterium replicates and reduces the growth rate of infected mycobacterium.[59] To combat the survival pressure of apoptosis, many successful pathogens encode genes whose products inhibit apoptosis in host cells, thus maintaining the viability for pathogen replication.[60] Although these mechanisms have been well studied in mammals, little is known about bacterial inhibition of apoptosis in fish. In our study, *V. harveyi* induced autophagy plays a role in pre-apoptotic stages and blocks the apoptotic signaling. Apoptosis and autophagy both promote and antagonize each other. In pre-apoptotic stages, cells block the apoptotic pathway and reduce the level of apoptosis through autophagy, thus maintaining the advantage. Autophagy does not trigger cell death in the early stages of apoptosis, but also promotes cell survival.[61] Autophagy during the late stage of apoptosis may promote apoptosis, and then the increased apoptosis inhibits the occurrence of autophagy through the migration of p53 and BH3 pathway.[62] The biological process is tightly regulated, including the interaction of autophagy and apoptosis. Numerous regulatory genes are involved in the interactive response mechanism of apoptosis and autophagy, Beclin-1 being one of them.[63] In addition to the regulation of autophagy initiation, Beclin-1 is also involved in regulating apoptosis.[45,64] Studies have shown that Beclin-1 loses its ability to resist apoptosis after being cleaved by activated caspases.[65] This suggests that Beclin-1 plays an important role as a "molecular switch" in the regulation of autophagy and apoptosis.

V. harveyi is a marine gram-negative bacterium that poses a serious threat to the health of marine aquaculture fisheries. *V. harveyi* infection causes meningitis and encephalitis in fish,[66] and *V. harveyi* infection causes cerebral congestion in grouper.[67] In response to bacterial infection, the innate immune and inflammatory responses are the main defense systems of fish. However, bacteria have also evolved the ability to evade immunity in symbiosis with their hosts. In summary, our results reveal a mechanism of *V. harveyi* immune evasion in fish. ACKR4a induces autophagy to inhibit NF-κB signaling and block apoptosis, which in turn facilitates *V. harveyi* infection in teleost fish. This is also the first time that gram-negative bacteria have been found to evade immunity by simultaneously regulating innate immunity and apoptosis via autophagy. This study provides insights into understanding the effects of autophagy on host-bacterium interaction in teleost fish and provides a perspective on mammalian resistance to bacterial infection.

Limitations of the study

In this study, we proved that *V. harveyi* induces ACKR4a directly binds the Beclin-1 and initiate autophagy to evade immunity. The detailed molecular mechanism behind Beclin-1 inhibiting apoptosis still remains to be further investigated.

STAR★METHODS

Detailed methods are provided in the online version of this paper and include the following:

SUPPLEMENTAL INFORMATION

Supplemental information can be found online at https://doi.org/10.1016/j.isci.2023.106105.

ACKNOWLEDGMENTS

This study was supported by the National Natural Science Foundation of China (31822057).

AUTHOR CONTRIBUTIONS

T.X. conceived and designed the study. Y.C., B.C., and W.Z. recruited subjects, collected the data, and worked on the analysis. Y.C. performed experiments, analyzed the samples, and interpreted the results. T.X. and Y.C. wrote the manuscript. All authors reviewed and approved the manuscript before submission.

DECLARATION OF INTERESTS

The authors declare that they have no conflict of interest.

Received: September 17, 2022
Revised: December 3, 2022
Accepted: January 27, 2023
Published: February 1, 2023

REFERENCES

1. Dinarello, C.A. (2018). Overview of the IL-1 family in innate inflammation and acquired immunity. Immunol. Rev. *281*, 8–27.
2. Gaidt, M.M., Ebert, T.S., Chauhan, D., Ramshorn, K., Pinci, F., Zuber, S., O'Duill, F., Schmid-Burgk, J.L., Hoss, F., Buhmann, R., et al. (2017). The DNA inflammasome in human myeloid cells is initiated by a STING-cell death program upstream of NLRP3. Cell *171*, 1110–1124.e18.
3. Xiao, T.S. (2017). Innate immunity and inflammation. Cell. Mol. Immunol. *14*, 1–3.
4. Koropatnick, T.A., Engle, J.T., Apicella, M.A., Stabb, E.V., Goldman, W.E., and McFall-Ngai, M.J. (2004). Microbial factor-mediated development in a host-bacterial mutualism. Science *306*, 1186–1188.
5. Janeway, C.A. (1989). Approaching the asymptote? Evolution and revolution in immunology. Cold Spring Harb. Symp. Quant. Biol. *54*, 1–13.
6. Vallabhapurapu, S., and Karin, M. (2009). Regulation and function of NF-κB

transcription factors in the immune system. Annu. Rev. Immunol. *27*, 693–733.

7. Krakauer, T. (2019). Inflammasomes, autophagy, and cell death: the trinity of innate host defense against intracellular bacteria. Mediators Inflamm. *2019*, 2471215.

8. Hurley, J.H., and Young, L.N. (2017). Mechanisms of autophagy initiation. Annu. Rev. Biochem. *86*, 225–244.

9. He, X., Zhu, Y., Zhang, Y., Geng, Y., Gong, J., Geng, J., Zhang, P., Zhang, X., Liu, N., Peng, Y., et al. (2019). RNF34 functions in immunity and selective mitophagy by targeting MAVS for autophagic degradation. EMBO J. *38*, 1009788–e101018.

10. Yin, L., Lv, M., Qiu, X., Wang, X., Zhang, A., Yang, K., and Zhou, H. (2021). IFN-Γ manipulates NOD1-mediated interaction of autophagy and Edwardsiella piscicida to augment intracellular clearance in fish. J. Immunol. *207*, 1087–1098.

11. Mansilla-Pareja, M.E., Bongiovanni, A., Lafont, F., and Colombo, M.I. (2017). Alterations of the coxiella burnetii replicative vacuole membrane integrity and interplay with the autophagy pathway. Front. Cell. Infect. Microbiol. *7*, 112.

12. Bravo-Santano, N., Ellis, J.K., Mateos, L.M., Calle, Y., Keun, H.C., Behrends, V., and Letek, M. (2018). Intracellular Staphylococcus aureus modulates host central carbon metabolism to activate autophagy. mSphere *3*, 003744–003818.

13. Winchell, C.G., Dragan, A.L., Brann, K.R., Onyilagha, F.I., Kurten, R.C., and Voth, D.E. (2018). Coxiella burnetii subverts p62/sequestosome 1 and activates Nrf2 signaling in human macrophages. Infect. Immun. *86*, e00608–e00617.

14. Lee, H.K., Lund, J.M., Ramanathan, B., Mizushima, N., and Iwasaki, A. (2007). Autophagy-dependent viral recognition by plasmacytoid dendritic cells. Science *315*, 1398–1401.

15. Jounai, N., Takeshita, F., Kobiyama, K., Sawano, A., Miyawaki, A., Xin, K.Q., Ishii, K.J., Kawai, T., Akira, S., Suzuki, K., and Okuda, K. (2007). The Atg5 Atg12 conjugate associates with innate antiviral immune responses. Proc. Natl. Acad. Sci. USA. *104*, 14050–14055.

16. Schaaf, M.B.E., Keulers, T.G., Vooijs, M.A., and Rouschop, K.M.A. (2016). LC3/GABARAP family proteins: autophagy-(un)related functions. FASEB J *30*, 3961–3978.

17. Chen, Z., Wang, T., Liu, Z., Zhang, G., Wang, J., Feng, S., and Liang, J. (2015). Inhibition of autophagy by MiR-30A induced by Mycobacteria tuberculosis as a possible mechanism of immune escape in human macrophages. Jpn. J. Infect. Dis. *68*, 420–424.

18. Kubori, T., Bui, X.T., Hubber, A., and Nagai, H. (2017). Legionella RavZ plays a role in preventing ubiquitin recruitment to bacteria-containing vacuoles. Front. Cell. Infect. Microbiol. *7*, 384.

19. Danial, N.N., and Korsmeyer, S.J. (2004). Cell death: critical control points. Cell *116*, 205–219.

20. Salvesen, G.S., and Ashkenazi, A. (2011). Snapshot: caspases. Cell *147*, 476–476.e1.

21. Zhou, Z.J., and Sun, L. (2016). Edwardsiella tarda-induced inhibition of apoptosis: a strategy for intracellular survival. Front. Cell. Infect. Microbiol. *6*, 76.

22. Günther, S.D., Fritsch, M., Seeger, J.M., Schiffmann, L.M., Snipas, S.J., Coutelle, M., Kufer, T.A., Higgins, P.G., Hornung, V., Bernardini, M.L., et al. (2020). Cytosolic Gram-negative bacteria prevent apoptosis by inhibition of effector caspases through lipopolysaccharide. Nat. Microbiol. *5*, 354–367.

23. Wierzbicki, I.H., Campeau, A., Dehaini, D., Holay, M., Wei, X., Greene, T., Ying, M., Sands, J.S., Lamsa, A., Zuniga, E., et al. (2019). Group A streptococcal S protein utilizes red blood cells as immune camouflage and is a critical determinant for immune evasion. Cell Rep. *29*, 2979–2989.e15.

24. Chen, J., Lu, Y., Ye, X., Emam, M., Zhang, H., and Wang, H. (2000). Current advances in Vibrio harveyi quorum sensing as drug discovery targets. Eur. J. Med. Chem. *207*, 112741.

25. Kimura, T., Jain, A., Choi, S.W., Mandell, M.A., Schroder, K., Johansen, T., and Deretic, V. (2015). TRIM-mediated precision autophagy targets cytoplasmic regulators of innate immunity. J. Cell Biol. *210*, 973–989.

26. Zlotnik, A., and Yoshie, O. (2012). The chemokine superfamily revisited. Immunity *36*, 705–716.

27. Ulvmar, M.H., Hub, E., and Rot, A. (2011). Atypical chemokine receptors. Exp. Cell Res. *317*, 556–568.

28. Bonecchi, R., Savino, B., Borroni, E.M., Mantovani, A., and Locati, M. (2010). Chemokine decoy receptors: structure-function and biological properties. Curr. Top. Microbiol. Immunol. *341*, 15–36.

29. Comerford, I., Litchfield, W., Harata-Lee, Y., Nibbs, R.J.B., and McColl, S.R. (2007). Regulation of chemotactic networks by 'atypical' receptors. Bioessays *29*, 237–247.

30. Horuk, R., Chitnis, C.E., Darbonne, W.C., Colby, T.J., Rybicki, A., Hadley, T.J., and Miller, L.H. (1993). A receptor for the malarial parasite Plasmodium vivax: the erythrocyte chemokine receptor. Science *261*, 1182–1184.

31. Bonini, J.A., Martin, S.K., Dralyuk, F., Roe, M.W., Philipson, L.H., and Steiner, D.F. (1997). Cloning, expression, and chromosomal mapping of a novel human CC-chemokine receptor (CCR10) that displays high-affinity binding for MCP-1 and MCP-3. DNA Cell Biol. *16*, 1249–1256.

32. Nibbs, R.J., Wylie, S.M., Yang, J., Landau, N.R., and Graham, G.J. (1997). Cloning and characterization of a novel promiscuous human beta-chemokine receptor D6. J. Biol. Chem. *272*, 32078–32083.

33. Burns, J.M., Summers, B.C., Wang, Y., Melikian, A., Berahovich, R., Miao, Z., Penfold, M.E.T., Sunshine, M.J., Littman, D.R., Kuo, C.J., et al. (2006). A novel chemokine receptor for SDF-1 and I-TAC involved in cell survival, cell adhesion, and tumor development. J. Exp. Med. *203*, 2201–2213.

34. Gosling, J., Dairaghi, D.J., Wang, Y., Hanley, M., Talbot, D., Miao, Z., and Schall, T.J. (2000). Cutting edge: identification of a novel chemokine receptor that binds dendritic cell- and T cell-active chemokines including ELC, SLC, and TECK. J. Immunol. *164*, 2851–2856.

35. Hall, R.A., Premont, R.T., and Lefkowitz, R.J. (1999). Heptahelical receptor signaling: beyond the G protein paradigm. J. Cell Biol. *145*, 927–932.

36. Brzostowski, J.A., and Kimmel, A.R. (2001). Signaling at zero G: G-protein-independent functions for 7-TM receptors. Trends Biochem. Sci. *26*, 291–297.

37. Sun, Y., Huang, J., Xiang, Y., Bastepe, M., Jüppner, H., Kobilka, B.K., Zhang, J.J., and Huang, X.Y. (2007). Dosage-dependent switch from G protein-coupled to G protein-independent signaling by a GPCR. EMBO J. *26*, 53–64.

38. Nibbs, R.J.B., and Graham, G.J. (2013). Immune regulation by atypical chemokine receptors. Nat. Rev. Immunol. *13*, 815–829.

39. Lewis, B.P., Burge, C.B., and Bartel, D.P. (2005). Conserved seed pairing, often flanked by adenosines, indicates that thousands of human genes are microRNA targets. Cell *120*, 15–20.

40. Friedman, R.C., Farh, K.K.H., Burge, C.B., and Bartel, D.P. (2009). Most mammalian mRNAs are conserved targets of microRNAs. Genome Res. *19*, 92–105.

41. Denli, A.M., Tops, B.B.J., Plasterk, R.H.A., Ketting, R.F., and Hannon, G.J. (2004). Processing of primary microRNAs by the Microprocessor complex. Nature *432*, 231–235.

42. Chen, Y., Cao, B., Zheng, W., Sun, Y., and Xu, T. (2022). eIF3k inhibits NF-κB signaling by targeting MyD88 for ATG5-mediated autophagic degradation in teleost fish. J. Biol. Chem. *298*, 101730.

43. Chu, Q., Sun, Y., Cui, J., and Xu, T. (2017). Inducible microRNA-214 contributes to the suppression of NF-κB-mediated inflammatory response via targeting myd88 gene in fish. J. Biol. Chem. *292*, 5282–5290.

44. Gay, N.J., Symmons, M.F., Gangloff, M., and Bryant, C.E. (2014). Assembly and localization of Toll-like receptor signalling complexes. Nat. Rev. Immunol. *14*, 546–558.

45. McKnight, N.C., and Zhenyu, Y. (2013). Beclin 1, an essential component and master regulator of PI3K-III in health and disease. Curr. Pathobiol. Rep. *1*, 231–238.

46. Mutwiri, G., Gerdts, V., Lopez, M., and Babiuk, L.A. (2007). Innate immunity and new adjuvants. Rev. Sci. Tech. *26*, 147–156.

47. Buchmann, K. (2014). Evolution of innate immunity: clues from invertebrates via fish to mammals. Front. Immunol. *5*, 459.

48. Chu, Q., Sun, Y., Cui, J., and Xu, T. (2017b). MicroRNA-3570 modulates the NF-κB pathway in teleost fish by targeting MyD88. J. Immunol. *198*, 3274–3282.

49. Yan, X., Zhao, X., Huo, R., and Xu, T. (2020). IRF3 and IRF8 regulate NF-κB signaling by targeting MyD88 in teleost fish. Front. Immunol. *11*, 606.

50. Takeuchi, O., Hoshino, K., and Akira, S. (2000). Cutting edge: TLR2-deficient and MyD88-deficient mice are highly susceptible to Staphylococcus aureus infection. J. Immunol. *165*, 5392–5396.

51. Keszei, A.F.A., Tang, X., McCormick, C., Zeqiraj, E., Rohde, J.R., Tyers, M., and Sicheri, F. (2014). Structure of an SspH1-PKN1 complex reveals the basis for host substrate recognition and mechanism of activation for a bacterial E3 ubiquitin ligase. Mol. Cell Biol. *34*, 362–373.

52. Günster, R.A., Matthews, S.A., Holden, D.W., and Thurston, T.L.M. (2017). SseK1 and SseK3 type III secretion system effectors inhibit NF-κB signaling and necroptotic cell death in salmonella-infected macrophages. Infect. Immun. *85*, e00010–e00017.

53. Mazurkiewicz, P., Thomas, J., Thompson, J.A., Liu, M., Arbibe, L., Sansonetti, P., and Holden, D.W. (2008). SpvC is a Salmonella effector with phosphothreonine lyase activity on host mitogen-activated protein kinases. Mol. Microbiol. *67*, 1371–1383.

54. Saitoh, T., and Akira, S. (2010). Regulation of innate immune responses by autophagy-related proteins. J. Cell Biol. *189*, 925–935.

55. Orvedahl, A., Alexander, D., Tallóczy, Z., Sun, Q., Wei, Y., Zhang, W., Burns, D., Leib, D.A., and Levine, B. (2007). HSV-1 ICP34.5 confers neurovirulence by targeting the Beclin 1 autophagy protein. Cell Host Microbe *1*, 23–35.

56. Kyei, G.B., Dinkins, C., Davis, A.S., Roberts, E., Singh, S.B., Dong, C., Wu, L., Kominami, E., Ueno, T., Yamamoto, A., et al. (2009). Autophagy pathway intersects with HIV-1 biosynthesis and regulates viral yields in macrophages. J. Cell Biol. *186*, 255–268.

57. Niu, H., Xiong, Q., Yamamoto, A., Hayashi-Nishino, M., and Rikihisa, Y. (2012). Autophagosomes induced by a bacterial Beclin 1 binding protein facilitate obligatory intracellular infection. Proc. Natl. Acad. Sci. USA. *109*, 20800–20807.

58. Hussain, M.A., Datta, D., Singh, R., Kumar, M., Kumar, J., and Mazumder, S. (2019). TLR-2 mediated cytosolic-Ca2+ surge activates ER-stress-superoxide-NO signalosome augmenting TNF-α production leading to apoptosis of Mycobacterium smegmatis-infected fish macrophages. Sci. Rep. *9*, 12330.

59. Lee, J., Hartman, M., and Kornfeld, H. (2009). Macrophage apoptosis in tuberculosis. Yonsei Med. J. *50*, 1–11.

60. McCormick, A.L. (2008). Control of apoptosis by human cytomegalovirus. Curr. Top. Microbiol. Immunol. *325*, 281–295.

61. Kuma, A., Hatano, M., Matsui, M., Yamamoto, A., Nakaya, H., Yoshimori, T., Ohsumi, Y., Tokuhisa, T., and Mizushima, N. (2004). The role of autophagy during the early neonatal starvation period. Nature *432*, 1032–1036.

62. Mariño, G., Niso-Santano, M., Baehrecke, E.H., and Kroemer, G. (2014). Self-consumption: the interplay of autophagy and apoptosis. Nat. Rev. Mol. Cell Biol. *15*, 81–94.

63. Furuya, D., Tsuji, N., Yagihashi, A., and Watanabe, N. (2005). Beclin-1 augmented cis diamminedichloroplatinum induced apoptosis via enhancing caspase 9 activity. Exp. Cell Res. *307*, 26–40.

64. Pattingre, S., Tassa, A., Qu, X., Garuti, R., Liang, X.H., Mizushima, N., Packer, M., Schneider, M.D., and Levine, B. (2005). Bcl-2 antiapoptotic proteins inhibit Beclin 1-dependent autophagy. Cell *122*, 927–939.

65. Djavaheri-Mergny, M., Maiuri, M.C., and Kroemer, G. (2010). Cross talk between apoptosis and autophagy by caspase-mediated cleavage of Beclin 1. Oncogene *29*, 1717–1719.

66. Grimes, D.J., Gruber, S.H., and May, E.B. (1985). Experimental infection of lemon sharks, Negaprion brevirostris (Poey), with Vibrio species. J. Fish. Dis. *8*, 173–180.

67. Mohamad, N., Mohd Roseli, F.A., Azmai, M.N.A., Saad, M.Z., Md Yasin, I.S., Zulkiply, N.A., and Nasruddin, N.S. (2019). Natural concurrent infection of *Vibrio harveyi* and *V. alginolyticus* in cultured hybrid groupers in Malaysia. J. Aquat. Anim. Health *31*, 88–96.

STAR★METHODS

KEY RESOURCES TABLE

REAGENT or RESOURCE	SOURCE	IDENTIFIER
Antibodies		
Rabbit anti-Miiuy croaker MyD88	This paper	N/A
Rabbit anti-ACKR4	CUSABIO	Cat# CSB-PA001411
Mouse anti-Flag	Beyotime	Cat# AF519;RRID:AB_2895204
Mouse anti-Tubulin	Beyotime	Cat# AT819
Mouse anti-HA	Beyotime	Cat# AH158;RRID:AB_2895203
Mouse anti-Myc	Beyotime	Cat# AM926;RRID:AB_2895205
Mouse anti-Cy3	Beyotime	Cat# A0521;RRID:AB_2923334
Rabbit anti-FITC	Beyotime	Cat# A0562;RRID:AB_2923335
Rabbit anti-p65	Beyotime	Cat# AF0246;RRID:AB_2923151
Rabbit anti-phospho-p65	Beyotime	Cat# AF5881
Rabbit anti-Bcelin-1	Boster	Cat# PB9076
Rabbit anti-LC3II	Boster	Cat# BM4827
Bacterial and virus strains		
Vibrio harveyi	This paper	N/A
Chemicals, peptides, and recombinant proteins		
DAPI	Beyotime	Cat# C1002
Critical commercial assays		
Lipofectamine RNAiMAX	Invitrogen	Cat# 13778150
Lipofectamine 3000	Invitrogen	Cat# L3000015
FastQuant RT Kit	Tiangen	Cat# KR106-03
BCA Protein Assay kit	Beyotime	Cat# P0012S
Caspase-Glo 3/7 Assay Kit	Promega	Cat# G8090
Endotoxin-Free Plasmid DNA Miniprep Kit	Tiangen	Cat# DP118
SYBR Premix Ex Taq™	Takara	Cat# DRR041S
Deposited data		
RNA sequencing	This paper	GenBank accession number: PRJNA845825
Experimental models: Cell lines		
MKC	This paper	N/A
MLC	This paper	N/A
MBrC	This paper	N/A
EPC	ATCC	Cat# CRL-2872
HEK 293	ATCC	Cat# CRL-3216
Experimental models: Organisms		
Miiuy croaker (~50 g, five-months-old, male or female)	This paper	N/A
Oligonucleotides		
Primers are listed in Table S1	This paper	N/A

(*Continued on next page*)

Continued

REAGENT or RESOURCE	SOURCE	IDENTIFIER
Recombinant DNA		
pcDNA3.1-Flag/HA/Myc	This paper	N/A
PGL3 Basic (or the mutant)	This paper	N/A
Software and algorithms		
DNAMAN	LynnonBiosoft	https://www.lynnon.com/
GraphPad Prism 8	GraphPad Software	https://www.graphpad.com
ImageJ	NIH, USA	https://imagej.nih.gov/ij

RESOURCE AVAILABILITY

Lead contact

Further information and requests for resources should be directed to and will be fulfilled by the lead contact, Tianjun Xu (tianjunxu@163.com).

Materials availability

All materials generated in this study are available from the lead contact without restriction.

Data and code availability

- The High-throughput sequencing data reported in this paper have been submitted to GenBank with accession number: PRJNA845825.
- This paper does not report original code.
- Any additional information required to reanalyze the data reported in this paper is available from the lead contact upon request.

EXPERIMENTAL MODEL AND SUBJECT DETAILS

Ethics and animals

All animal experimental procedures were performed in accordance with the National Institutes of Health's Guide for the Care and Use of Laboratory Animals, and the experimental protocols were approved by the Research Ethics Committee of Shanghai Ocean University (No. SHOU-DW-2018-047). Miiuy croaker (~50 g, five-months-old, sex-randomized) was obtained from Zhoushan Fisheries Research Institute, Zhejiang Province, China. Fish was acclimated in aerated seawater tanks at 25°C for six weeks before experiments. Animals were then randomly selected for study.

Cell line

M. miiuy brain cells (MBrC), *M. miiuy* kindey cells (MKC), and *M. miiuy* liver cells (MLC) were cultured in L-15 medium (HyClone) supplemented with 15% fetal bovine serum (FBS; Gibco), 100 U/ml penicillin, and 100μg/ml streptomycin at 26°C. The above cell lines were prepared from the corresponding tissues of the miiuy croaker. Tissues were minced thoroughly with scissors and pushed carefully through a 100-μm nylon mesh in L-15 medium containing penicillin (100 IU/ml), streptomycin (100 mg/ml), 2% fetal bovine serum (FBS), and heparin (20 units/ml) to give a single cell suspension. The filtered cell suspension was loaded onto 34/51% Percoll (Pharmacia, USA) density gradient, and then centrifuged at 400 × g for 40 minat 4°C. Subsequently, the supernatant was removed and the cells at the interfaces were obtained with care and washed twice in L-15 medium at 300 × g for 10 minat 4°C. Cells were cultured in L-15 containing 0.1% FBS at 26°C, 4% CO_2. The cell pellet was re-suspended in fresh complete L-15 medium supplemented with 20% FBS in next day. HEK293 cells were cultured in Dulbecco's modified Eagle medium (GE, USA) supplemented with 10% fetal bovine serum (FBS) (Thermo Fisher Scientific, USA), 100 U mL−1 of penicillin, and 100 μg mL−1 of streptomycin at 37°C in 5% CO_2.

METHOD DETAILS

Bacterial infections

For *M. miiuy* challenge, 1ml of *Vibrio harveyi* (1.5×10^8 cfu/ml) was injected into *M. miiuy* through the intraperitoneal injection, and then tissues were collected at 48 h after challenge. For cells infection, cells was seed into 12-wells plate for 18h, the culture medium of cells was charged to L-15 without streptomycin and penicillin, and then cells were infected with live *V. harveyi* with MOI of 5 for short infection (no longer than 12h).

RNA isolation and real-time quantitative PCR

Total RNA was isolated with TRIzol reagent (Invitrogen) following the manufacturer's protocol. Afterward, the quality and concentration of total RNA were measured with Nanodrop 2000 (Thermo Fisher). cDNA was synthesized with HiScript III RT SuperMix for qPCR kit and Universal SYBR qPCR Master Mix (Vazyme) was used for qPCR according to the manufacturer's protocol. All samples were analyzed in triplicate and the expression values, unless indicated, were normalized to β-actin. Primers used for qPCR analysis are listed in Table S1. The procedure is as follows: 95°C for 3 min, 40 cycles of 95°C for 10s, 60°C for 10s, and 95°C for 15s.

Plasmids construction and transfection

ACKR4a was screen out based on previous RNA-seq data (GenBank accession number: PRJNA845825). The CDS of ACKR4a, Ap-1, and Beclin-1 were amplified from the *M. miiuy* cDNA through standard PCR methods, and then the expression plasmids were cloned into pcDNA3.1 with different tags. All the recombinant plasmid was confirmed by western blot and Sanger sequencing. The PROMO database was used to predict the transcription factors of ACKR4a, and different mutants were constructed based on the binding site positions of the screened transcription factors in the ACKR4a promoter region. The ACKR4a, ULK1, ATG5, and Beclin-1 promoter was amplified from *M. miiuy* genomic DNA through standard PCR methods, the wide-type and the mutants of ACKR4a promoter luciferase reporters were cloned into PGL3-Basic.

Transfection was carried out at a rate of 1.5 μl per 1μg of plasmid or 0.5nmol of siRNA according to the Lipofectamine 3000 (Thermo Fisher) instructions to ensure transfection efficiency.

Dual-Luciferase reporter assays

EPC cells were inoculated into 24-well plates at 50% density and transfected with the luciferase reporter gene plasmid when the density reached 70%. Cells were lysed at 24h post-transfected; supernatants were collected and measured following the Dual Luciferase Reporter Assay Kit (Vazyme) manufacturer's protocol. Each experiment was repeated in triplicate.

Immunoblot analysis

MBrC, MKC, and MLC cells were seed into 12-wells plate for 18h, and the transfection method was consistent with the above. The cell supernatant was collected with cell lysate at 48 hours post-transfected and the protein concentration was determined by the BCA Protein Assay kit. 50μg protein was subjected to SDS-PAGE followed by membrane transfer, antibody incubation, and ECL analysis.

RNA interference

The ACKR4a-targeted small interfering RNAs (ACKR4a-si), Ap-1-targeted small interfering RNAs (Ap-1-si), and Beclin-1-targeted small interfering RNAs (Beclin-1-si) were designed by the online website Thermo Fisher Scientific (http://www.thermofisher.com). The siRNAs and a nontargeting control siRNA (Ctrl-si) were purchased from Gene Pharma. ACKR4a-si is as follows: 5′-GAAACGCCTTAGTCGTGGCTGTCTA-3′. Beclin-1-si is as follows: 5′- CCTCTCAAGCTGGACACATCCTTCA-3′. Ap-1-si is as follows: 5′-CGGCC AAGATGGAGACTCCTTTCTA-3′.

Enzyme linked immunosorbent assay (ELISA)

Cells were stimulated with *V. harveyi* at 12h post-transfected, and then cells were collected and lysed. The ELISA assay was performed with the Fish TNFα ELISA kit (number MM-065502, MAISHA Industries) according to the manufacturer's protocol.

Colony-forming units (CFU) assay

After the cells were infected with *V. harveyi*, the culture medium was sucked, washed with PBS 4 times, digested with trypsin for 2-3 min, discarded the trypsin, blown down the cells with PBS, centrifuged at 1200 g for 5 min, removed the supernatant after centrifugation, added the cell lysate and mixed evenly, stood for 30 min, diluted 1,000 times and coated on the 2261E Agar (Hopebio) plate, cultured the plate at 26°C for 12 h and counted.

Cell apoptosis

Cell apoptosis was analyzed by flow cytometry at 48h post-transfection. 100 μL/well trypsin was added for 20s; cells were then collected according to the manufacturer's protocol and prepared with the Annexin V-FITC Apoptosis Kit (Beyotime). In brief, cells were stained with PI and Annexin-V-FITC, and the positively stained cells were counted using FACScan.

Immunofluorescence and confocal microscopic analysis

Cell culture slides (polylysine treated) were prepared and transfected. Cells were washed with PBS 3 times and then fixed with 4% paraformaldehyde at 24 hours post-transfected. After blocking with 0.5% FBS for 1 h, the primary antibody and the secondary antibody were added. Finally, after counterstaining with DAPI staining solution for 10 min, the cell culture slides were fixed with an anti-fluorescent bursting agent (Boster). Fluorescence signals were assessed by confocal microscopy (Leica).

Live cell imaging

Cells were transfected with GFP-MyD88, and grown on cell culture slides. Then cells were treated for 90min with the 50nM Lyso-Tracker Red DND-99 (Invitrogen). The cells were washed with PBS, and the cells were imaged with confocal microscopy (Leica).

Caspase activity assay

Cells were inoculated into 96-well plates and suffered different treatments. The caspase activity assay was performed according to the Caspase-Glo 3/7 Assay (Promega) manufacturer's protocol. In brief, 100μL/well of caspase 3/7 working solution was added and then incubates for 1h at 25°C, protected from light. The plate was centrifuged at 800 g for 2 min, with fluorescence intensity monitoring at Ex/Em = 490/525 nm with GloMax Navigator (Promega).

Coimmunoprecipitation (Co-IP) analysis

The cells were collected with RIPA (Beyotime) at 32 h post-transfection. 50 μL Agarose Protein A/G (Sigma) was washed three times with 1ml RIPA. After incubating Agarose Protein A/G with primary antibody for 2 h, the supernatant of cell lysates was added. These complexes were placed on a turntable mixer at 10rpm and incubated overnight at 4°C. After that, the beads were washed with cold PBS three times. All the steps need to be on the ice, and then beads were boiled at 95°C for 5 min, and proteins were separated by SDS-PAGE.

Cell proliferation

Cell proliferation assays were performed with BeyoClickEdU cell Proliferation Kit with AlexaFluor 488 (Beyotime) following the manufacturer's instructions. All the experiments were performed in triplicate.

Transcription factor prediction

The 5'-end sequence of ACKR4a was obtained and intercepted 2,000bp from the start codon, which was then analyzed by the JASPAR database to screen for possible transcription factor binding sites.

Chromatin immunoprecipitation (ChIP) assay

Cells were inoculated in 10cm^2 dishes and cells were treated differently after reaching 1×10^6, after which ChIP was performed. Briefly, cells were treated with 1% formaldehyde for 10 minat 37°C, followed by Glycine Solution for 5 minat 25°C to terminate the cross-linking. The cells were washed twice in PBS, lysed on ice, collected and ultrasonically fragmented. Centrifugation at 4°C, 12,000 rpm for 10min. The appropriate antibody was added to the supernatant and rotated for 12hat 4°C. The Agarose Protein A/G beads were added to it, at 4°C for 2h. Centrifuge at 6,000rpm for 5min and discard the

supernatant. Washed the beads in sequence with low salt wash buffer, low salt wash buffer, LiCl wash buffer, and TE buffer. Finally, the beads were eluted with elution buffer and diluted to 500μl with diffusion buffer. Added 5M NaCl at 65°C for 12h, 0.5M EDTA, 1M Tris-HCl, and 20mg/ml Proteinase K treated for 2h at 45°C.

QUANTIFICATION AND STATISTICAL ANALYSIS

The statistical analysis was performed using Student's two-tailed t-test (two groups of data were compared) and two-way ANOVA(more than two groups of data were compared). The date is represented as the mean ± SD of n independent experiments. Value of $p< 0.05$,*, was considered significant, $p< 0.01$,**, was considered highly significant.